TEAM VARUNA

SRI SAIRAM COLLEGE OF ENGINEERING

Anekal, Bangalore

MUTHUVEL A

MS (BY RESEARCH)

DEPARTMENT OF MECHNICAL ENGG.

(FACULTY ADVISOR)

DANANJAY (CAPTAIN)

ISMAIL

MOHAN KUMAR

ANISH

ASHRAF

INDEX

CHAPTER			TITLE	PAGE
1			**INTRODUCTION**	4
	1.1		Autonomous Underwater Vehicle (AUV)	4
2			**LITERATURE SURVEY**	6
3			**SHAPE & SIZE**	8
4 & 5			**WEIGHT AND BUOYANCY**	9
6			**FABRICATION**	9
	6.1		Polypropylene	9
		6.1.1	Use of polypropylene	9
	6.2		Properties	10
	6.3		Acrylic	10
	6.4		Optical clarity	10
	6.5		Resistance to aging	10
	6.6		Light weight	10
	6.7		Impact resistance	10
7			**COMPONENT PLACEMENT AND WEIGHT DISTRIBUTION**	10
	7.1		AUV symmetry about the three planes.	10
	7.2		The aligning moment ensures horizontal stability.	10
	7.3		Roll and pitch movement are neglected.	11
8			**CENTRE OF GRAVITY & BUOYANCY**	11
9			**DRAG CALCULATION AND COEFFICIENT OF DRAG**	11
	9.1		Computational domain	11
	9.2		Assembly of AUV and Domain	11
		9.2.1	Unstructured mesh	11
	9.3		Results and Analysis of Bare AUV	12
		9.3.1	Introduction	12
		9.3.2	Grid independent study	12
		9.3.3	Velocity contour and vector diagram	13
		9.3.4	Pressure contour diagram	13
10			**VEHICLE SPEED**	14
11			**Hull and Electronics Rack**	14
12			**Electrical system**	14
			Power Management System	15
13			**Electronic system**	15
	13.1		Nvidia Jetson TX1	16
	13.2		microcontrollers	16
		13.2.1	Arduino mega 2560	16

14			**SENSORS**	17
	14.1		Camera	17
		14.1.1	Kongberg OE 14- 376/377	
15			**Feedback**	18
16			**Movement control**	18
	16.1		Thrusters	18
	16.2		Motor driver	18
	16.3		DC voltage regulator	18
	16.4		Relay	19
17			**Switch**	19
	17.1		Launch switch	19
	17.2		Check switch	19
18			**Software**	19
	18.1		Vision processing	20
	18.2		Buoy dashing	20
	18.3		L space passing	21
19			**Programming**	21
	19.1		Torpedo launching programming	21
	19.2		Ball dropping programming	21
	19.3		Octagon exit	21
	19.4		Path finder	21
	19.5		Recovery algorithm	21
	19.6		Navigation	21
	19.7		Mission Planner	22
20			**CONCLUSION**	22
			REFERENCES	23

CHAPTER 1

INTRODUCTION

1.1 Autonomous Underwater Vehicle (AUV)

Flow over submerged body has been a subject of great number of investigation mainly because of wider engineering applications. Some examples are flow over car, buildings, flight-deck of a ship, underwater appended vessels like submarine, torpedo, Autonomous Underwater Vehicle (AUV), Remotely Operated Vehicle (ROV) etc. [1].

AUV is a free swimming marine robot that require little or no human intervention [1]. Underwater bodies are axis-symmetric or cylindrical like shapes [2]. They are compact, self-contained, low-drag profile. The vehicle uses on-board computers, power packs and vehicle payloads for navigation, automatic control, and guidance. They are also equipped with state-of-the-art scientific sensors to measure oceanic properties, or specialized biological and chemical payloads to detect marine life when in motion Fig. 1.1 and Fig. 1.2 shows typical AUV while Fig. 1.3 and Fig. 1.4 shows the details of the inside modules of AUV.

Fig 1.1 Deep – sea cruising AUV "Uramisha" [3]

Fig 1.2 An AUV model [4]

Fig 1.3 The interior arrangement of an AUV [4]

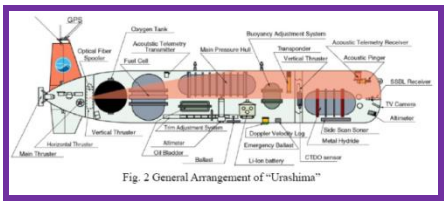

Fig 1.4 Diagram of the general arrangements in AUV "Urashima"[3]

Twenty years ago, development of autonomous underwater vehicles (AUVs) were in nascent stage, and there was little guidelines available to the designers in deciding the fundamental shape and size of their craft [5]. Since then, researchers have tried a wide variety of AUV shapes and sizes, like the National Oceanography Centre's (NOC) Auto sub and Hydroid's (Pocasset, Massachusetts) REMUS; laminar flow bodies, like the early Kongsberg Maritime (Kongsberg, Norway) HUGIN vehicles; streamlined rectangular styles, like Atlas Elektronik GmbH's (Bremen, Germany) Sea Otter etc.

Each of the different types of AUV came with a vision of fulfilling a certain set of requirements [5]. Fig.1.5 shows various AUVs built by different countries.

Autonomous Underwater Vehicles (AUVs) are established as a viable tool for Oceanographic explorations. Being independent, AUVs fill the gap in Ocean exploration left by the existing manned submersible and Remotely Operated Vehicles (ROV) technology. AUVs are attractive as cheaper and efficient alternatives to the older technologies and are breaking new ground in many applications. Fig.1.6 shows various applications of an AUV.

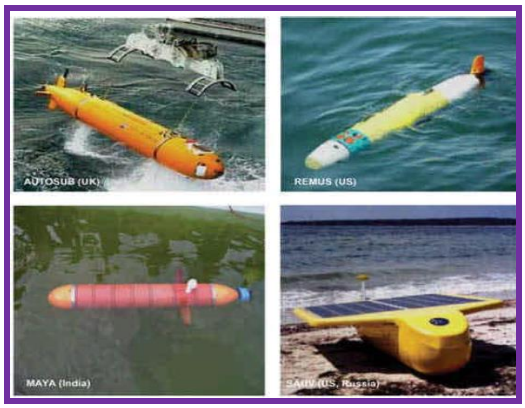

Fig 1.5 Various AUVs built by different countries [4]

As explained earlier, underwater bodies like AUV are axis symmetric or cylindrical in shapes. Building an underwater body is a complex task that requires many different areas of engineering expertise. This is because the ocean is the most challenging environment in the world. There are so many factors that must be considered when designing a vehicle to operate in such a harsh environment. Extreme pressures, water tight integrity, corrosion, surface and underwater currents, hydrodynamics and navigation are just a few of the many difficulties confronting an engineering team. Also, the issues of a faster cruising speed and a tighter turning radius are to be addressed by researchers [2]. One of the driving forces behind the hull design is the effect of drag on an underwater vehicle. An important parameter in fluid mechanics is the Reynolds number (Re). The Reynolds number (Re) for a typical AUV travelling at approximately 1 meter per second is ~1.0 x 10^5. At this Reynolds number the flow is generally turbulent [6].

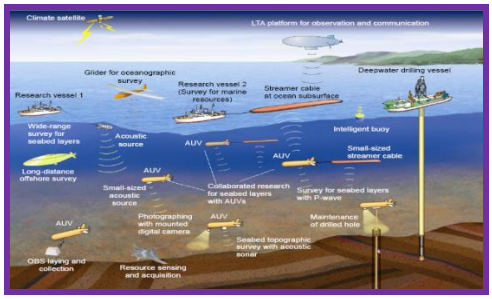

Fig 1.6 Various functions of the AUV

The effect of the shape and vehicle appendages on the hydrodynamic drag is harder to assess and has a significant impact on the performance of an AUV. The flow over an underwater appended vessel during level flight is characterized by the development of thick boundary layers, flow separation; flow into and through propeller, vortices formed at the root and tip of appendages and appendage turbulent wake [7]. The spatial non-uniformity and temporal fluctuations of flow into vessel propulsion unit significantly affect propulsion noise. The experimental analysis are very costly (due to its set up) and time consuming. Scaling up the results obtained from the model experiment to full scale may give rise to errors and detailed measurement is time consuming as well as costly[8]. AUVs are designed to operate over a range of glide slopes so that they can efficiently maintain geographic positions while profiling. Flow visualization studies carried out in the wind tunnel for different wind speeds and attack angles demonstrated that laminar flow separates just behind of the maximum diameter of the body and reattaches turbulently near the tail for attack angles as high as 12^0. There is a fear of increased turbulent flow, disrupted fore-body laminar flow, turbulent separation on the after section or instability in the flow regime. Analysing these problems using CFD is not only cheaper and takes lesser time than the model testing, but also is more accurate and efficient than the empirical methods. Accurate numerical prediction of the flow in the stern region of the hull both with and without the propeller operating is important to evaluate the after body thrust deduction, thus limiting the expensive resistance and self-propulsion model experiments in a towing tank[9]. The recent advances in CFD made it possible to predict the flow over the fully appended underwater bodies.

However, the prediction of flow field during manoeuvring is still challenging [10-12]. This is because the wake of manoeuvring underwater body is a highly complex three-dimensional flow field dominated by interactions of large-scale vertical structures from the separated flow around the body and trailing flow structures from the sail and various control surfaces. As the body progresses through a manoeuvre, the local flow angle changes in an unsteady manner further complicating the flow interactions. The complex interaction of various vortices structures represents a particular difficulty in the prediction of such flows. However, simulation of manoeuvring is important from the point of design and operational safety. The key requirement for manoeuvring simulations is the accurate prediction of the forces acting on the hull, propeller and control surfaces.

CHAPTER 2

LITERATURE SURVEY

A discussed earlier, AUVs are designed to operate over a range of glide slopes so that they can efficiently maintain geographic positions while profiling. Flow visualization studies carried out in the wind tunnel for different wind speeds and attack angles demonstrated that laminar flow separates just aft of the maximum diameter of the body and reattaches turbulently near the tail for attack angles as high as 12^{0}[6]. There is a fear of increased turbulent flow, disrupted fore body laminar flow, turbulent separation on the after section or instability in the flow regime.

JagadeshandMurali[13] made a comparative study of five turbulence models viz. AKN *k*-ε model, CHC *k*-ε model, YS *k*-ε model, Standard *k*-ε model and*k*-ε RNG model to investigate the hydrodynamic resistance of AUV. For the study the authors used 2-D axis symmetric model. Based on the study, they concluded that AKN *k*-ε model predicts the flow and near wall behaviour better than other models.

Jagadesh et al. [14] carried out both experimental and numerical investigations of hydrodynamic forces coefficient of 3-D AUV hull. The numerical investigation is carried out with AKN *k*-ε model incorporated in ANSYS Fluent software. Based on the study, the authors concluded that AKN *k*-ε model is well suited to predict the hydrodynamics forces acting on AUV hull.

Barros et al.[15] carried out a comparative study on CFD analysis, analytical and semi-empirical (ASE) method on MAYA AUV. For the CFD analysis, the authors used SST Menter*k*- ω model incorporated in Fluent and observed that the CFD analysis is able to predict the bare –Hull normal force and moment coefficients very well.

Amit Ray et al. [16] carried out CFD analysis of AUV bare – hull with Fluent software. For the analysis they used standard *k*-ε, Realizable *k*-ε, RNG *k*-ε, standard *k*- ω and SST *k*-ω model to find the hydrodynamics coefficients with various drift angles. Based on their study, the authors concluded that Realizable *k*-ε model predicts better than other models. The computed value of axial force is within 20% for a drift angle greater than 4 degrees.

Ting M.C et al.[17]carried out CFD analysis of underwater glider with FLUENT software. For the analysis they used Spalart-Allmaras turbulence model to find the hydrodynamic coefficients. They varied the angle of attack from -8^{o} to 8^{o}and observed that the lift and drag coefficients are increasing as the function of angle of attack. Wake formation occurs at the tail part and also at the junction part between main wing and fuselage body.

He Zhang et al.[18] carried out numerical simulation of AUV vehicle by CFD software Fluent to evaluate manoeuvrability of vehicles and the corresponding hydrodynamic coefficients. Based on the study, the authors concluded that the

computer simulation provides a low-cost reliable data for the hydrodynamic tests.

Chao-ho Sung et al.[19] carried out the numerical analysis of flow around a turning submarine by solving incompressible RANS equation in a steady rotating coordinate system. For the analysis they used standard k-ω and realizable k-ε models. The authors reported that the prediction of the forces is much better than the prediction of moments. They observed that for a symmetric body, the realizable k-ε model predicts the lift and pitching moment better than standard k-ω model and also give a consistently more accurate prediction of the flow around a turning submarine.

M. M. Karim et al.[20] carried out the analysis of 2-D axisymmetric flow around bare submarine hull using both structured and unstructured grid. Shear Stress Transport (SST) k-ω model is used to simulate turbulent flow past the hull surface. They observed that unstructured grid gives better result and flow visualization than the structured grid.

Jason Evans and Meyer Nahou[21] carried out the analysis of hydrodynamic forces acting on the hull and control plane for the full 360º angle of attack range. The model used to simulate is C-SCOUT AUV as a predictive design tool to evaluate and compare the performances of the two configurations.

Serge ToxopeusandGuilhermeVaz[22] carried out the analysis of un-appended DARPA SUBOFF model for several oblique inflow conditions using a single grid topology to reduce the amount of grid generation time. For large inflow angles the authors suggested the use of unsteady procedure with grid refinement for capturing the unsteady vortex shedding phenomena as it influences the flow field around the body and thereby the forces acting on it. Various numerical simulation approaches (boundary elements, panel methods, etc.) for studying marine propeller geometries have been used for decades, but only recently, due to the rapid advances in computer power and in the parallelization capabilities, different CFD methods, and in particular Reynolds Averaged Navier-Stokes (RANS) equation solvers, are increasingly applied to simulate the full three-dimensional viscous and turbulent flow for various propeller geometries [23–30]. Multi-block structured grids are also in greater use, particularly where commercial CFD codes (e.g. CFX4) offer this as a default methodology. In the USA, this approach is still followed along with finite analytic solver methods. However, although structured multi-block offers many advantages (retaining good quality grids and natural approaches to domain decomposition for parallel computing), they are not as flexible as unstructured or hybrid approaches for highly complex geometries. Fully unstructured grids were also used wherein particular regions of the flow domain are populated with regular, structured, finite volume cells in order to take advantages of efficiency and greater numerical accuracy. Fully unstructured grids are often subject to high overheads in data storage and solver speed. In addition, certain finite volume cell types are not best suited to boundary layer flows (e.g. tetrahedral). A combination of structured multi-block and unstructured methodologies would be ideal, but no suitable solvers were in existence. To a large extent, this deficiency has now been overcome. Unstructured methods have now been advanced to the stage where solvers are in use for cell volumes of almost arbitrary geometry (i.e. polyhedral). This allows very complex geometries to be modelled and enables mixtures of structured and unstructured grids to be used together since issues relating to the interfaces between regions can be solved using these arbitrary cell volumes [31-33]. The finite volume solvers used are formulated for their versatility rather than efficiency, but advances in computing speed and parallel architectures have more than compensated for this. The main concern

with such methods relates to the formal order of accuracy achieved, not simply by the originators, but by those using these methods in the commercial environment.

CHAPTER 3

MECHANICAL DIVISION - SHAPE & SIZE

3.1 Hull Design

The hull of AUV houses the electrical systems and it is waterproofed. The hull, needs to have enough space for the electrical systems (for future expansion), should have a good accessibility, needs to be corrosion resistant, has to be able to withstand high impact and at the same time needs to be capable of withstanding the water pressure. A cylindrical shape is chosen for the hull because it has a favourable geometry for both pressure and dynamic reasons, at the same time it offers also enough room for the electrical systems. The hull is made out of a thick acrylic tube which keeps the hull relatively cheap, corrosion free and able to withstand an impact. The acrylic tube is closed with aluminium plate with propylene cap at one end and another end is covered by hemispherical propylene cap. The cap consists of an aluminium ring which is permanently fixed to the hull with connectors in the aluminium plate. Sealing between the ring and the plug is ensured by an O-ring, Sealing is provided in the axial direction of the acrylic tube which means that water pressure will ensure more tension on the sealing area when the vehicle is submerged, since the water pressure will press the end caps against the acrylic tube. The camera, which is mounted inside the hull, can deliver an underwater view. The transparent acrylic tube is also useful to see warning lights of the central processing unit from outside the hull.

The AUV has an overall length of 60cm and a maximum height and depth of 40cm each. The rear view, side view, bottom view and Isometric view of AUV are show in Fig. 3.1 to Fig. 3.4. The Exploded view of the AUV is show in Fig. 7.1 and Fig. 7.2.

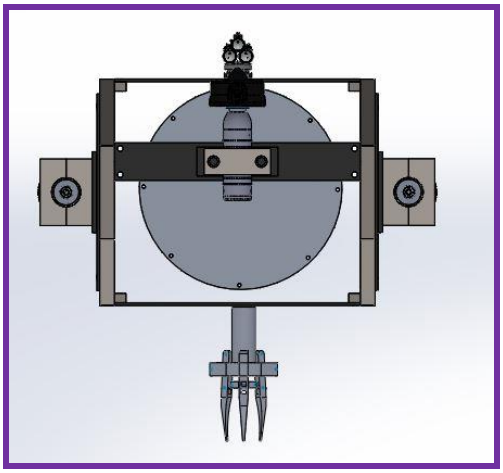

Fig.3.1 Rear View of the AUV

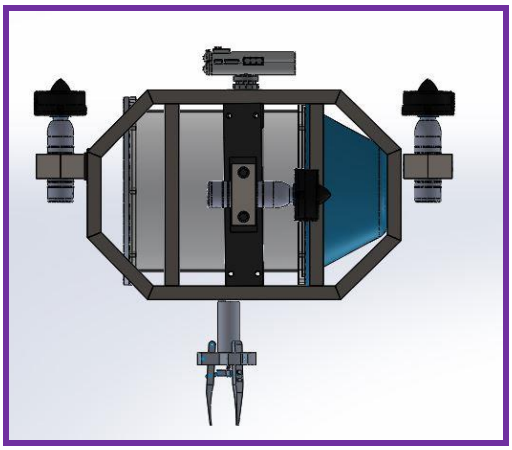

Fig.3.2 Side View of the AUV

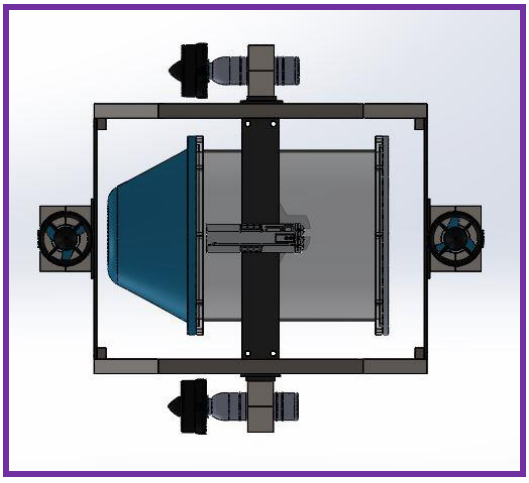

Fig.3.3 Top View of the AUV

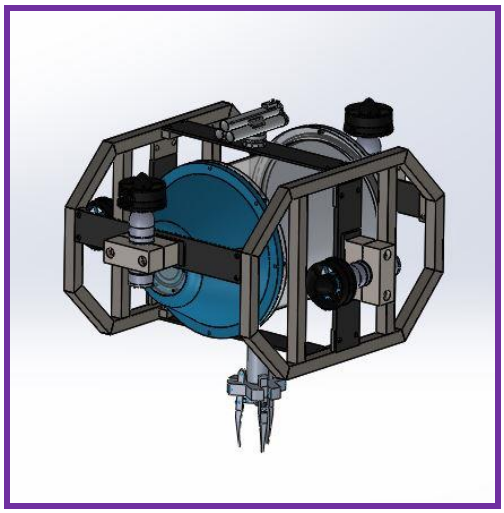

Fig.3.4 Isomeric view of the AUV

CHAPTER 4 AND 5

WEIGHT AND BUOYANCY

$$Weight = Desnsity\ of\ Material(\rho) \times Volume\ of\ Material(v) \times Acceleration\ due\ to\ Graivty(g)$$

....(4.1)

$$Buoyancy\ Force = Density\ of\ fluid(\rho) \times Volume\ of\ Water\ Displaced \times acceleration\ due\ to\ gravity(g)$$

....(4.2)

Sl. No.	Parts	Weight (N)	Buoyancy (N)
1	Frame	269.60	60.09
2	Acrylic Hull	36.97	283.41
3	Thrusters	15	7
4	Battery	10	-
5	Grabber	8	10
6	Torpedo Launcher	7	9
	Total	**351.57**	**369.5**

Table. 3.1. Buoyancy Calculation

The AUV buoyancy system is based on a dynamic diving method. This method requires the AUV to be slightly positively buoyant, vertically mounted thrusters will then control the depth of the AUV. A drawback of this method is the large energy consumption the system will need to control depth since thrusters must remain powered to keep the AUV submerged. An advantage of this system is that when the thrusters are switched off buoyancy will ascend the vehicle, which means that the vehicle will surface itself when there are electrical problems. Other advantages of this method lay in the economic reasoning, for example, there are no complex sealing methods needed for depth control.

CHAPTER 6

FABRICATION

Our hull is made up of 4 major materials i.e. Steel, Aluminium, Polypropylene and Acrylic. The main frame of the AUV is made up of steel. It will give rigid shape to our AUV. It will withstand more than 50m. For placing our electronics materials, we are using tubes with the thickness of 10mm for and 35cm diameter. We made the hemisphere shape in the bow part for reducing the drag and the aluminium disc is used for closing the rear part. The flange is used for connecting rear and front by the screws. All the process is made by welding, milling, grinding, facing etc.

6.1. Polypropylene

Polypropylene is a type of thermoplastic polymer resin. The chemical designation is C_3H_6.

6.1.1 Why do we use Polypropylene?

- It does not absorb water like other plastics.
- It does not mould or otherwise deteriorates in the presence of bacteria, mould or other elements.

- It is unlikely to shatter and will take significant damage prior to breaking, though it is not as sturdy as other plastics such as polyethylene.
- It is lightweight and very flexible.

6.2. The properties

- Low density (weight saving).
- High stiffness.
- Heat resistance.
- Chemical inertness.
- Steam barrier properties (food protection)
- Good transparency.
- Good impact/rigidity balance.
- Stretch ability (film and fiber applications).

6.3. Acrylic

It is a transparent thermoplastic often used in sheet form as a lightweight or shatter-resistant alternative to glass.

6.4 Optical Clarity

Clear cast acrylic has a remarkable 93% transparency rate. This means that it is one of the clearest materials available. It can also be chemically welded together to form a solid piece with no noticeable seams and no reduction in transparency. This gives acrylic amazing light transmission properties.

Glass, on the other hand, tends to take on a greenish colour the thicker it is made and multiple panes can only be connected using adhesive, which leaves highly visible seam.

6.5 Resistance to Aging

Acrylic is essentially resistant to aging, meaning that it will look just as clear in ten years as it does today. The reason is because cast acrylic is unaffected by sunlight or fluorescent lighting.

6.6 Light weight

While glass can be heavy, acrylic is noticeably lighter. In fact, acrylic weighs half as much as glass. This makes clear cast acrylic the preferred choice for overhead signs and other applications where weight needs to be taken into consideration.

6.7 Impact Resistance

Acrylic tubes have seventeen times greater impact resistance to glass. Acrylic sheets have two to three times more impact resistance than double strength window glass and four to five times the impact resistance of wire glass and several other types of glass. Unlike glass, acrylic is also shatter resistant and extremely resilient to a variety of temperatures and conditions.

CHAPTER 7

COMPONENT PLACEMENT AND WEIGHT DISTRIBUTION

7.1 AUV symmetry about the three planes

The AUV is symmetric about the x-z plane and close to symmetric about the y-z plane. Although the AUV is not symmetric about the x-y plane it is assumed that the vehicle is symmetric about this plane, so one able to decouple the degrees of freedom. The AUV can be assumed to be symmetric about three planes since the vehicle operates at relatively low speed.

7.2 The aligning moment ensures horizontal stability

The AUV remains close to horizontal in all manoeuvres and stabilizes itself, since the centre of gravitation and centre of buoyancy are correctly in right order aligned (i.e. aligning moment). This

could be concluded from underwater videos made during underwater experiments.

7.3 Roll and pitch movement are neglected

The roll and pitch movement of the AUV are passively controlled and can, therefore, be neglected, since the AUV stabilizes itself due to the aligning moment. Therefore, the corresponding parameters need not have to be identified.

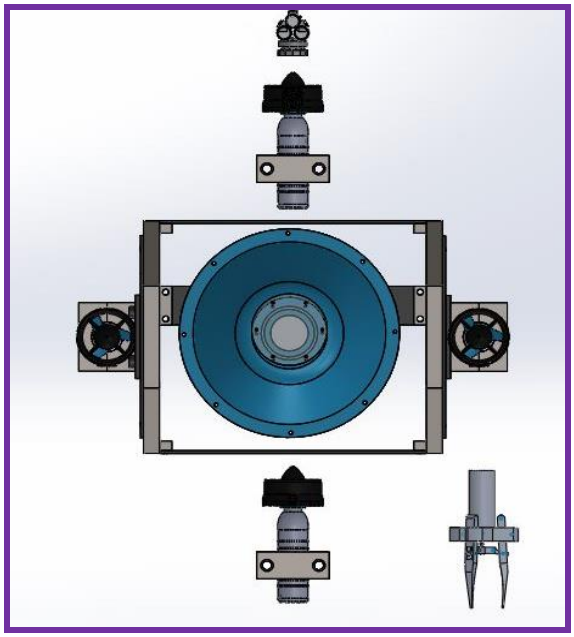

Fig.7.1 Exploded front view of the AUV

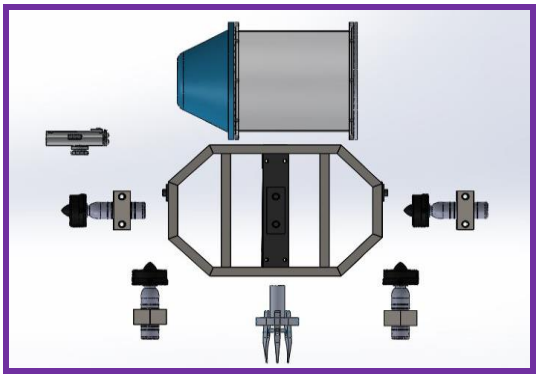

Fig.7.2 Exploded Side view of the AUV

CHAPTER 8

CENTRE OF GRAVITY & BUOYANCY

The Centre of gravity of the AUV is

(Xg, Yg, Zg) = (0.0m, 0.0m, 0.5m)

The Centre of Buoyancy of the AUV is

(Xb, Yb, Zb)= (0.0m, 0.16m, 0.0m)

CHAPTER 9

CALCULATION AND COEFFICIENT OF DRAG

9.1 Computational domain

The computational domain is modelled, based on the specifications given in Fig. 9.1.

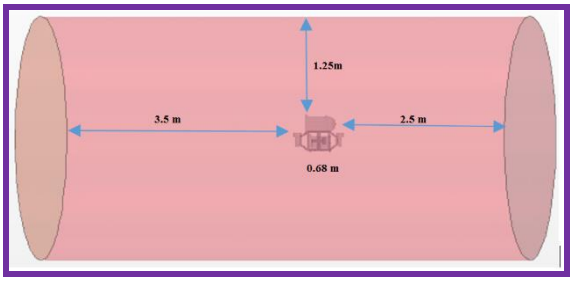

Fig 9.1 Specifications for Computational Domain

9.2 Assembly of AUV and Domain

The assembly of the AUV and Domain is done in STAR-CCM+. The two models are imported into the software and the AUV volume is subtracted from the Domain volume. Thus, the two separate volumes become one volume with the domain as the negative volume.

9.2.1 Unstructured mesh

In unstructured mesh, polyhedral mesh was chosen as it gives more accuracy for lesser number of cells, thus the computational time is reduced. During generation of the meshes, attention is given for refining the meshes near the AUV so that the boundary layer can be resolved properly. The typical mesh for AUV and domain is shown in Fig 9.2 and a magnified view near the solid wall of AUV is shown in Fig 9.3

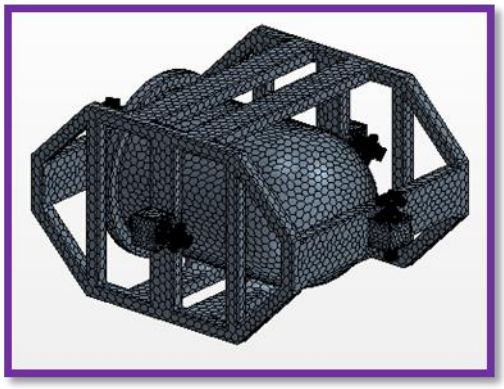

Fig. 9.2 Section view of AUV and Domain with unstructured mesh

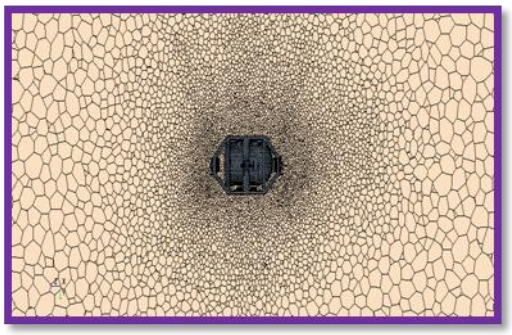

Fig 9.3 Unstructured mesh - magnified view near the wall

9.3. RESULTS AND ANALYSIS OF BARE AUV

9.3.1 Introduction

Three-dimensional numerical analysis of the flow over **A**utonomous **U**nderwater **V**ehicle (AUV) is carried out with the general-purpose **R**eynolds **A**veraged **N**avier-**S**tokes **E**quations (RANSE) solver STAR-CCM+. For the analysis the DARPA SUBOFF model has indicated in Chapter 4 is taken for the analysis simulating the towing tank testing carried out by Roddy, R. F. Steady analysis is carried out both with unstructured polyhedral meshes with AKN k-ε turbulence models for bare AUV.

For all the cases, the maximum residual from continuity, x-momentum, y-momentum and z-momentum is restricted to 10^{-6} as convergence criteria. Initially, 300 iterations are carried out with first-order upwind scheme and relaxation factor for velocity as 0.3 and pressure as 0.1 to guard against divergence of the solution. Later, till the convergence criteria are met, iterations are carried out with second-order upwind scheme with velocity relaxation factor as 0.5 and pressure relaxation factor as 0.3 to obtain higher accuracy and also to accelerate the convergence.

Sl. No.	Turbulence models	Drag Force (N)
1.	AKN k-ε	67.54
2.	V2f k-ε	68.46
3.	Standard Low Re	76.44
4.	EB model	71.61

Table 9.1. Drag Force for various Turbulence models

Following data were considered for the analysis:

- Liquid = H_2O (Water)
- Density (ρ) = 1000.0 kg/m^3 (for water)

The value of turbulent kinetic energy at the inlet is calculated as follows

$$k = \frac{3}{2}(T_i * u)^2 \qquad \ldots (7.1)$$

Where,

T_i – turbulent intensity = 0.0515 Js/kg-m

The value of dissipation rate (ε) for k-ε model and specific dissipation rate (ω) for k-ω model at the inlet are calculated from:

$$\varepsilon = \frac{k^{3/2}}{0.7 \times L} \qquad \ldots (7.2)$$

9.3.2Grid independent study

Grid independent test is carried out with 0.35 million, 0.5 million and 0.67million cells for 0.5 m/sec velocity. AKN k-ε turbulence model is used for the test. The difference between the values obtained for 0.5 million cells and 0.67 million cells is very less (less than 2%). Hence, 0.67 million cells are considered for further analysis as shown in

Table 9.2. Drag force for various speeds is shown in Table 9.3. Drag force for various turbulence model is shown in Table 9.4.

Sl. No.	No. of Grids (Millions)	Drag Force (N)
1.	0.50	69.89
2.	0.59	67.54
3.	0.71	66.92

Table 9.2 Grid independent study

Sl. No.	Velocity (m/sec)	Drag Force (N)
1.	0.1	0.67
2.	0.5	16.86
3.	0.8	43.66
4.	1	67.54

Table 9.3 Drag force for various speed

Sl. No.	Turbulence models	Drag Force (N)
1.	AKN k-ε	67.54
2.	V2f k-ε	68.46
3.	Standard Low Re	76.44
4.	EB model	71.61

Table 9.4 Drag force for various turbulence models

9.3.3 Velocity contour and vector diagram

The velocity contour diagram for AKN k-ε turbulence model is shown in Fig. 9.4

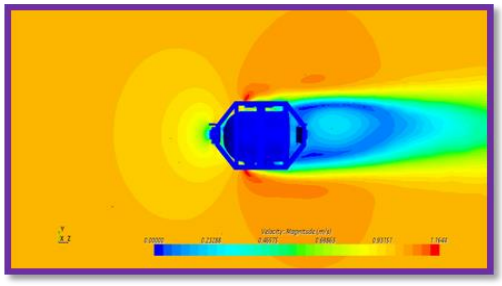

Fig.9.4 Velocity contour for AKN k-ε turbulence model

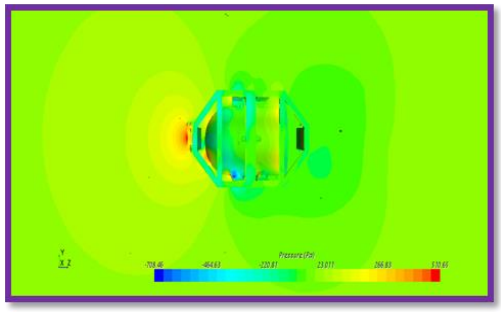

Fig. 9.5 Pressure contour for AKN k-ε turbulence model

From the velocity contour diagram, the variation of the velocity of flow over the AUV has seen. At the bow of the AUV, stagnation condition has clearly captured. Also, boundary layer formation is seen near the walls. A s the flow advances over the body, the velocity increases gradually and then reduces in the cap region due to curvilinear nature of the cap geometry as shown in Figure 9.5.

9.3.4 Pressure contour diagram

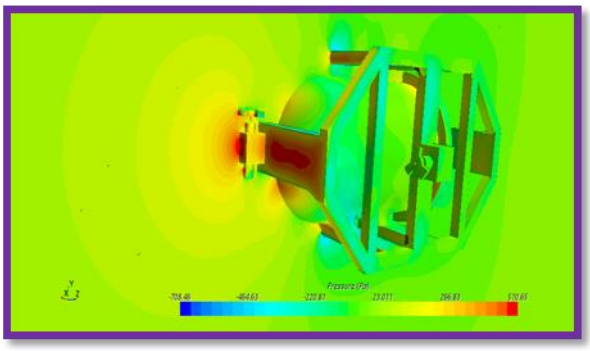

Fig.9.6 Pressure contour for AKN k-ε turbulence model

From the Pressure contour diagram, the variation of the velocity of flow over the AUV has seen. At the bow of the AUV, stagnation condition has clearly

captured. Also, boundary layer formation is seen near the walls. As the flow advances over the body, the velocity increases gradually and then reduces in the cap region due to curvilinear nature of the cap geometry in starboard side and bow side of the AUV as shown in fig 9.6, Fig 9.7 and Fig 9.8.

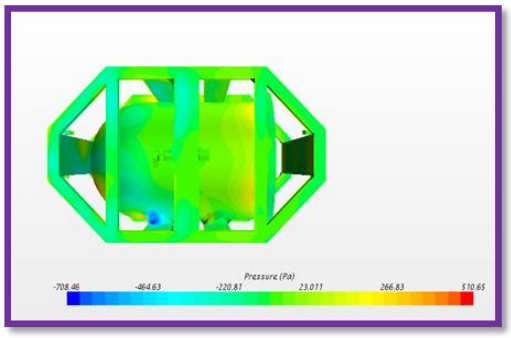

Fig. 9.7 Pressure contour on the starboard side

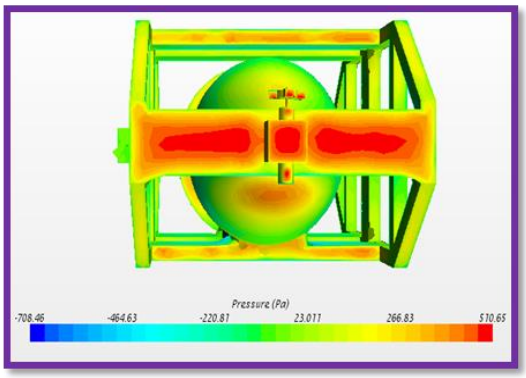

Fig. 9.8 Pressure contour on the bow side

CHAPTER 10

VEHICLE SPEED

Relatively low speed, hence the lift forces can be neglected. The AUV operates at relative low speed, i.e. max. 0.5 m/s, which means that lift forces can be neglected. The low speed was verified during underwater experiments (wet tests).

CHAPTER 11

HULL AND ELECTRONICS SYSTEMS

11.1 Hull and electronics rack

The hull of AUV houses the electrical systems and it is water proofed. The hull, needs to have enough space for the electrical systems (for future expansion), should have a good accessibility, needs to be corrosion resistant, has to be able to withstand high impact and at the same time needs to be capable of withstanding the water pressure. A cylindrical shape is chosen for the hull because it has a favorable geometry for both pressure and dynamic reasons, at the same time it offers enough room for the electrical systems. The hull is made up of a thick acrylic tube which keeps the hull relatively cheap, corrosion free and able to withstand an impact. The acrylic tube is closed with aluminum plate with propylene cap at one end and another end is covered by hemispherical propylene cap. The cap consists of an aluminum ring which is permanently fixed to the hull with connectors in the aluminum plate. Sealing between the ring and the plug is ensured by an O-ring, Sealing is provided in the axial direction of the acrylic tube which means that water pressure will ensure more tension on the sealing area when the vehicle is submerged, since the water pressure will press the end caps against the acrylic tube. A camera, which is mounted inside the hull, can deliver an underwater view. The transparent acrylic tube is also useful to see warning lights of the central processing unit from outside the hull.

The hull surrounds the electronics rack. These racks are so effectively designed to attach and carry all electronics board and components. The effective design helps us to reduce the wires and connectors.

CHAPTER 12

ELECTRICAL SYSTEM

VARUNA's electrical system provides the vehicle with power and an interface between the on-board computer and the other electronic devices. Nearly

all boards are populated in-house. We designed a back panel which allows us to improve wire management for electrical interfaces between boards inside the hull.

12.1 Power management system

The power management system of VARUNA has been designed intelligently to run for more than 40 minutes. Four thruster and all other electronics equipment used in VARUNA is powered by 5 number of 7.4V 10000mAh 25C LiPo battery. 4 batteries are used for the four thrusters where as other 1 battery for other electrical peripherals. The current and voltage across batteries, thrusters and other electrical peripherals are regularly monitored through adequate sensors and the data is stored in the storage disk.

All incoming power to the vehicle is routed through the merge board, which combines up to two power sources to provide single power rail for the vehicle. The merge board draws from all batteries equally to ensure they are discharged evenly.

VARUNAs power management system is well equipped with a kill switch. The microcontroller is connected with all the sensors and it will off the entire power source of the AUV whenever it faces any fault in the system.

EUIPMENTS	Voltage(V)	Amp(A)
OE 14376	12	350
At mega 2560	12	500
DFF-3d	12	1400
W-MK-17020-3	10	1500
NVIDIA JETSON	5.5	350
10 DOV IMU sensor	6	50
1000kv motor	7.2	10000
DVL 500	10	400

Table12.1 Power Distribution

And the Total power=**110900**

Therefore, the maximum power consumed will be 150 watts

We thereby deciding to use the batteries of following specification **12v & 18AH**

Total running duration- battery AH/total current consuming

i.e,18/12.5 = 1.4 Hrs

12.2 Actuators

These provide the mechanism which is used to hold the given object. These consist of spring a mechanism which is controlled by the controlling circuits.

12.3 Torpedo Launcher

It is a cylindrical shape tube for launching torpedo. This is similar to that of the play gun which consists of spring mechanisms for launching the torpedo which is intern controlled by the microcontroller circuits.

12.4 Grabber

To complete tasks involving dropping ball and shifting objects we designed a special grabber. This is located in the vehicles bottom plane and represents a servo in a waterproof casing, which controls a hook bar. This hook is planned to be used for grabbing objects and dropping ball.

For projecting the ball inside we will use actuators arm made up of rubber and plastic.

CHAPTER 13

ELECTRONIC SYSTEM

Electronics are required in the AUV to make it capable of solving the mission tasks autonomously and effectively. The architecture has been designed

to be modular enough to integrate different sensors and devices according to the specific requirements.

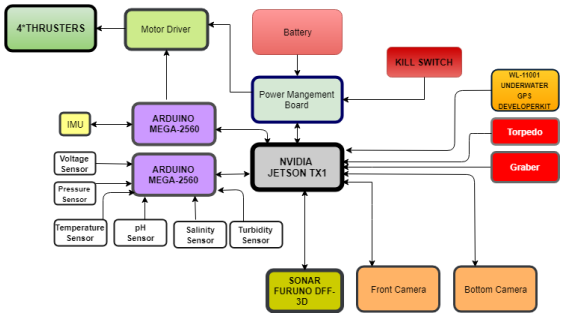

Fig.13.1: Electronics system communication diagram

13.1 NVIDIA JETSON TX1

This technology breakthrough gives you the performance and power efficiency to create next-generation products targeting GPU computing, computer graphics, and artificial intelligence (AI). Jetson TX1 provides a variety of standard hardware interfaces that can be exposed using a carrier board, enabling a highly flexible and extensible platform. It's the ideal solution for all your use cases that demand high computational performance in a low-power envelope. The module is supported by NVIDIA's complete development tool chain, including a variety of common APIs. The Jetson SDK, Jetpack, includes a Linux BSP and sample file system for your device, developer tools, and libraries for AI, Computer, Multimedia, and Graphics, supporting documentation, and code samples to help us to get started.

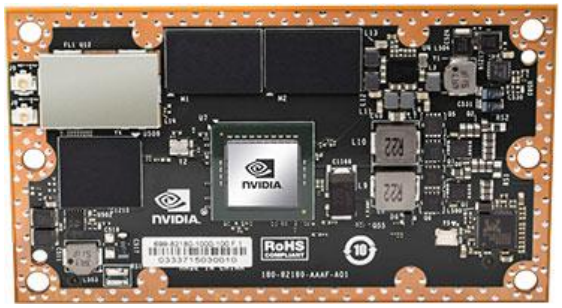

Fig.13.1 Nvidia Jetson TX1 board

TECHNICAL SPECIFICATIONS

Jetson TX1 System-on-Module

- GPU- 1 TFLOP/s 256-core Maxwell
- CPU- 64-bit quad-core ARM A57 CPUs
- Memory -4 GB LPDDR4 | 25.6 GB/s
- Storage- 16 GB eMMC
- Networking- 10/100/1000Mbit Ethernet
- Camera -12 CSI DPHY 1.1 lanes Dual ISP, 1.5 Gb/sec
- Display- Dual pipeline HDMI/ eDP/DSI
- Video -4K 60 Hz decode 4K 30 Hz encode
- USB -USB 3.0 + USB 2.0 PCIE Gen 2 1x1 + 1x4 (full x4 slot)
- Size -87 mm x 50 mm
- Weight- (incl. TTP) 88 g

13.2 Microcontrollers

VARUNA use two different type of microcontroller. The 2 Arduino Mega-2560 is chosen to be the main controller of the AUV the main power switch on the AUV respectively

13.2.1 Arduino Mega 2560

Fig. 13.2: Arduino mega2560

The Arduino Mega2560 is the main microcontroller used in VARUNA. This board is connected with

the main computer via USB cable. Being directed by the main on-board computer it takes logic inputs from IMU, pressure sensor and other peripherals, executes the code and hence accordingly controls the thrusters'. This enables the main computer to focus on extensively image processing and mission tasks.

It is engaged in accomplishing tasks in real time: receiving and controlling operation units, computing controlling and stabilizing regulators, controlling thrusters as well as monitoring temperature, pressure, water leak and other parameters inside the main hull. Selection of Arduino Mega2560 is determined by its good processing speed energy saving and plentiful peripherals needed to handle sensors and thrusters.

Technical specification

- Microcontroller – AT mega 2560
- Operating Voltage- 5V
- Input Voltage (recommended)- 7-12V
- Input Voltage (limits) -6-20V
- Digital I/O Pins 54 (of which 14 provide PWM output)
- Analog Input Pins -16
- DC Current per I/O Pin -40 Ma
- DC Current for 3.3V Pin- 50 Ma
- Flash Memory 256 KB of which 8 KB used by boot loader
- SRAM- 8 KB
- EEPROM- 4 KB
- Clock Speed- 16 MHz

CHAPTER 14

SENSORS

VARUNA is well equipped with different sensors and 2pixy cameras or Kongsberg OE 14 – 376/377 cameras. The following sensors provide feedback to the microcontroller:

14.1CAMERA

14.1.1 Kongsberg OE 14 – 376/377 cameras

For making image processing based controlling the AUV we used two Kongsberg OE 14 – 376/377 cameras. These 2 cameras are place inside the hull, one camera placed in front of the hull and another one place down side of the hull. So, we get a complete update of all detected objects' positions every 20ms. The 2 OE 14 are connected with Nvidia Jetson TX1 board. This camera can detect color.

Fig.14.1: Kongsberg camera

Technical specs

- Performance Horizontal Resolution 480 TVL/PH
- Light Sensitivity 100 mV video at 20 x 10-3 lux faceplate
- 350 mV video at 90x10-3 lux faceplate
- Minimum Scene Illumination 0.28 lux
- Signal to Noise Ratio >56 dB (weighted)
- Electrical Scan Standard 625 lines 50Hz
- PAL (OE14-376) 525 lines 60Hz NTSC (OE14-377)
- Sensor Elements 752 (H) x 582 (V) (OE14-376) 768 (H) x 492 (V) (OE14-377)

- Video Output 1V pk –pk composite video, into 75Ω
- Power Input 12 to 24 V dc, 220mA (350mA max), with LEDs turned on
- Light Output 99 lux at 1 meter
- Optical Lens 4.3 mm, F1.8
- AOV in water Horizontal: 36° Vertical: 27.5° Diagonal: 43.5°
- Iris Control CCD Electronic
- Focus Range 300mm to Infinity, Fixed

CHAPTER 15

FEEDBACK

The feedback from the sensors through microcontroller reaches the main on-board computer over a serial line where it is stored in the micro Sd card. The data stored is used after the mission to monitor the system characteristics and for debugging purposes.

CHAPTER 16

MOVEMENT CONTROL

VARUNA content four KZ-720B underwater thruster. These thrusters are responsible for keep AUV underwater and movement.

16.1Thruster

The AUV is propelled by 4 KZ-720B underwater thruster brush DC motor. The thrusters run on 6V DC supply, consuming maximum continuous current of 7A they can produce 0.72Kg of maximum thrust's One thruster placed in front of the AUV and another one back of the AUV to keep the AUV under the water. Another two thrusters two side of the AUV is to move the vehicle forward and reverse as well as right and left too.

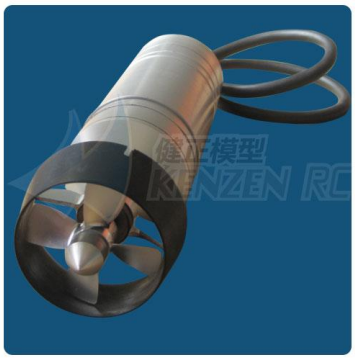

Fig.16.1: KZ-720B Thrusters

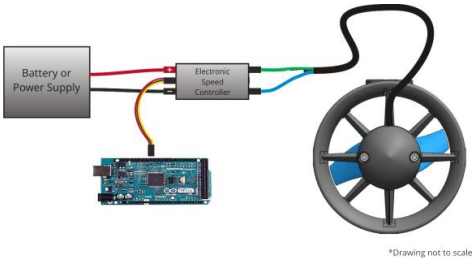

Fig.16.2: Arduino with Thrusters control

16.2 Motor driver

To control the four kenzen thrusters we used 4 Hercules lite motor drivers. The 6V-36V, 8Amp motor driver can take up to 30A peak current load and can be operated up to 10 KHz PWM. The motor driver is used under/over voltage, over temperature and short.

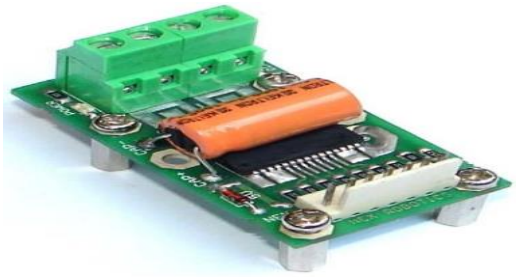

Fig.16.3: Hercules lite motor driver

16.3 DC Voltage Regulator:

The electronic equipment's in the AUV are connected with a dc voltage regulator which gives 5V continuous power supply to all the electronics peripherals.

16.4 Relay

A relay is an electrically operated switch. Current flowing through the coil of the relay creates a magnetic field which attracts a lever and changes the switch contacts. The coil current can be on or off so relays have two switch positions and they are double throw (changeover) switches. We are using 6V DC relay to complete our circuit. These relays used as switch between batteries and components. The concept kill switch is depending on a relay.

CHAPTER 17

SWITCH

17.1 Launch Switch

A RFID RC-522 with RF RC card-based switching system is made for VARUNA launch. The RFID tag in conjunction with the RF RC card is used for switchless launch for the AUV. The reader interfaced with the microcontroller. The relay serves as an interface between the power source and electronic system. The program in the Arduino board will determine the appropriate outputs activating the relay and switch on the power for AUV.

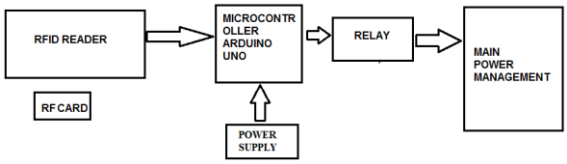

Fig.17.1: Block diagram for launch.

17.2 Check Switch

The main microcontroller is Arduino Mega2560 is connected with all the sensors and thrusters. The voltage sensor and current sensor always check the flow of voltage and current through the thrusters and power supply. With the help of IMU we are able to control and stable the AUV. When the power switch will on the microcontroller will check all the connections and the main CPU for any error. If any error occurs the microcontroller will kill the power supply of the AUV. This check switch helps us to protect the electronics component from any damage.

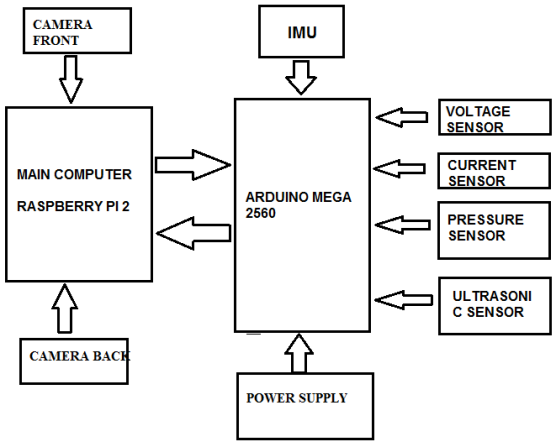

Fig.17.2: Block diagram for check switch

CHAPTER 18

SOFTWARE

VARUNA's software architecture is designed by the software team. The software on the vehicle is powered by a NVidia Jetson TX1 Board. With the help of Open CV-Python (Open Source Computer Vision) the coding is done in NVidia Board. Open CV-Python is a library of Python bindings designed to solve computer vision problems.

Python is a general-purpose programming language very popular mainly because of its simplicity and code readability. It enables us to express ideas in fewer lines of code without reducing readability.

Compared to languages like C/C++, Python is slower. Python can be easily extended with C/C++, which allows us to write computationally intensive

code in C/C++ and create Python wrappers that can be used as Python modules. This gives us two advantages: first, the code is as fast as the original C/C++ code (since it is the actual C++ code working in background) and second, it easier to code in Python than C/C++. OpenCV-Python is a Python wrapper for the original Open CV C++ implementation.

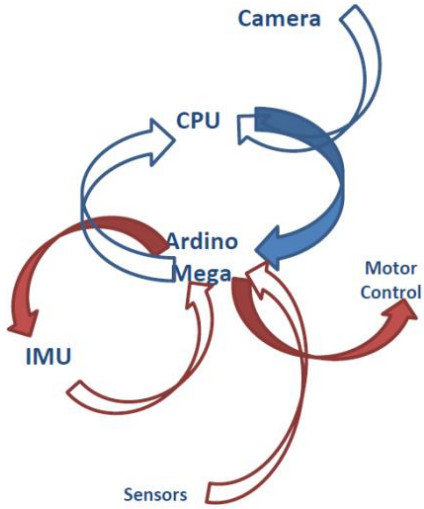

The software system is implemented as one stack with different packages representing various modules like vision, navigation and mission planning. The modules are entirely independent of the internal implementations of each other.

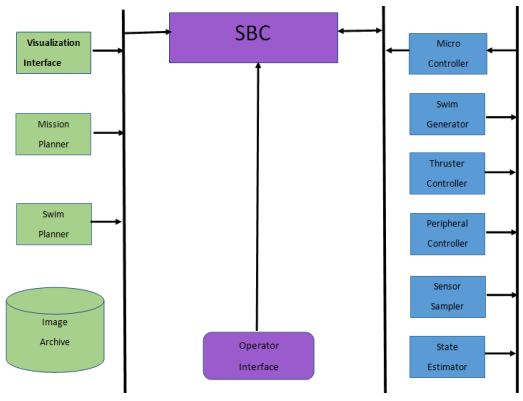

Fig.18.1 Software Architecture

18.1 VISSION PROCESSING:

VARUNA's vision system is equipped with 2 cameras front and bellow the hull which helps us to make an image processing-based control system. That can detect different objects, colour of objects and colour lines. It uses a hue-based colour filtering algorithm to detect objects. Since It uses hue (colour), the object needs to have a distinct hue. It can identify 7 different colours. We teach the camera for those different colour objects underwater. Based on different distances placed objects the camera was programmed to measure distance also. 2 cameras are connected with the SBC. The front camera is used to detect various objects like the buoy, L shape, hearten and the dropper. The other camera is placed at the bottom of the AUV in the second support rod. In the task of ball dropper, this camera is used to find the bowl placement and position the AUV such that the ball drops exactly in it. The detection is one of the most computationally expensive levels and since not all the modules are required at any given moment, but still have to be working in order to accumulate evidences, priorities are assigned by the algorithm based on the current mission.

18.2 Buoy dashing

When the AUV attains its normalized position at a depth in water, it then searches for the colour buoy through the front camera.

This task algorithm is done easily by pixy camera. Pixy module searches for the colour of red, yellow or green which is defined as per the competitions requirements. When SBC find the correct colour buoy by the Pixy then AUV reset to the appropriate location and orientation and starts to move towards it and finally passes over the buoy.

18.3 L space passing

For this task, we will be using the shape detection algorithm of Pixy camera which will be detecting the L shaped rods. Pixy programmed with lot of images. These images are using opencv functions then used for detecting and passing the L shaped gate.

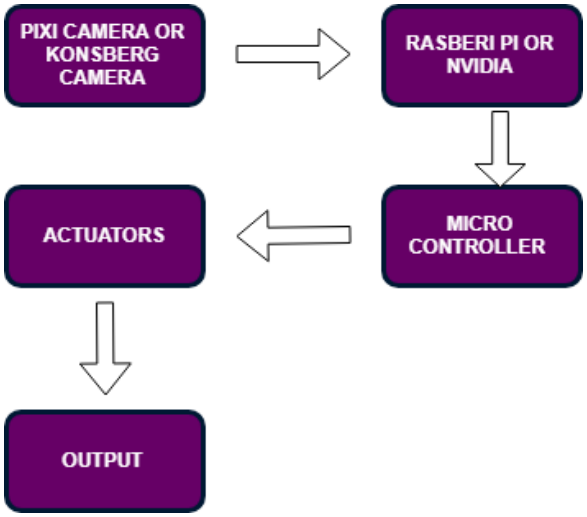

Fig.18.2: Launching layout

CHAPTER 19

PROGRAMMING

19.1 Torpedo launching programming

This task too uses the same mechanism of training and using the classifier for detecting the heart in shape. When detected, control is sent to the launch function through the serial line for the release of the torpedo.

19.2 Ball dropping programming

Camera on the bottom of the AUV is used for this task. With pixy object detection algorithm, it searches bin to which the ball has to drop. Once detected the algorithm repositions the AUV itself such that, when the ball is dropped, it falls in the bowl which is pre-induced in the algorithm.

19.3 Octagon exit

After dropping the ball, the front camera in the AUV is used to track the bottom of the octagon and move towards it. Then with the help of bottom camera it centres the mark such that when the AUV rises it comes out thought the octagon as whole.

19.4 Path finder

At certain position AUV is in need to find the path that is kept below. The bottom camera is used to identify the rectangular orange path with the help of colour detection algorithm. It follows it in the front direction with is decided by the magnetometer from the IMU to reach the corresponding next task.

19.5 Recovery algorithm

VARUNA is implemented with a recovery system, such that in the situation of error or incorrect movement, the navigational system with imaging is used to recover to the last know “good path” which is determined by the localization algorithm. IMU plays a major role in recovery as it is one of the important inputs to the recovery algorithm.

19.6 Navigation

VARUNA uses four thrusters to maintain its movement and keep it underwater. Two thrusters are placed front and back of AUV and run in same speed for keep the vehicle underwater and maintain same level. Two thrusters are placed at both sides of the AUV to provide thrust for moving the vehicle along the X-axis and the Y-axis. For turning the AUV in a particular direction the RPM of one thruster will be regulated through a computer program. For sudden turn it may off one side thrusters or slow the speed. With a 10 DOF IMU Module we can navigate our AUV. It is a combination of 3 axis gyroscope, 3 axis accelerometer, 3 axis magnetometer MPU 9255,

and a barometric digital pressure sensor BMP 280. Data from IMU is used to determine the YAW angle of the vehicle and maintain the vehicle's balance through ROLL and PITCH values.

19.7 Mission Planner

The mission planner is responsible for running and controlling the various missions that VARUNA performs. Each mission has a completion and/or timeout time. Whenever a completion condition has been reached, the current mission terminates and VARUNA moves the next mission. If a mission is taking too long and reaches its timeout then the mission planner terminates it and moves on. Because of this is done so that VARUNA does not spend too much time on a single mission without getting a chance to perform the other missions.

Each mission has various parameters which are all stored in main storing device that are automatically reloaded when changed.

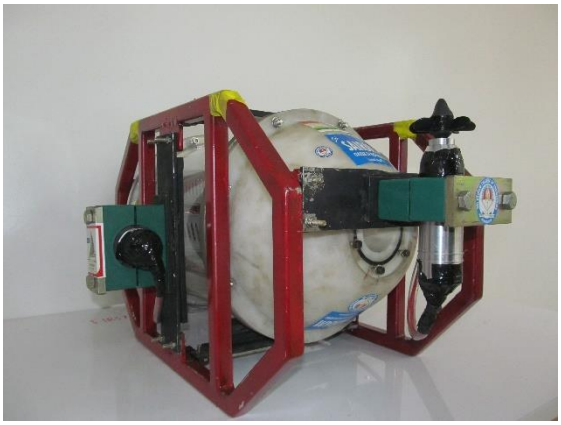

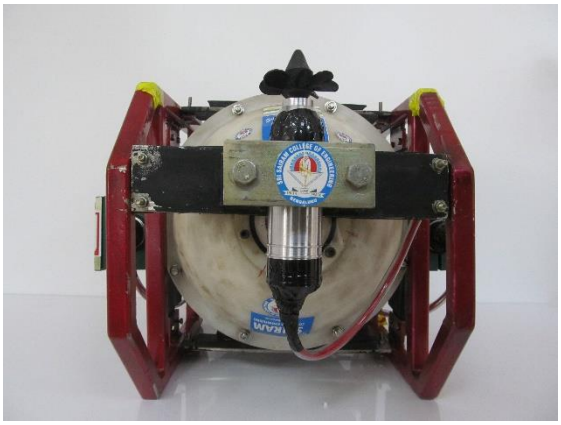

CHAPTER 20

CONCLUSION

In this project, analysis is carried out for POSEIDON model of AUV with commercial code STAR-CCM+. Both Structural and Flow Analysis has carried out for bare AUV propeller interaction for various drift angles. In the analysis, AKN k-ε model (buffer layer turbulence models are used for the CFD analysis The Drag coefficient, the FOS, stress, strain, etc. are presented.

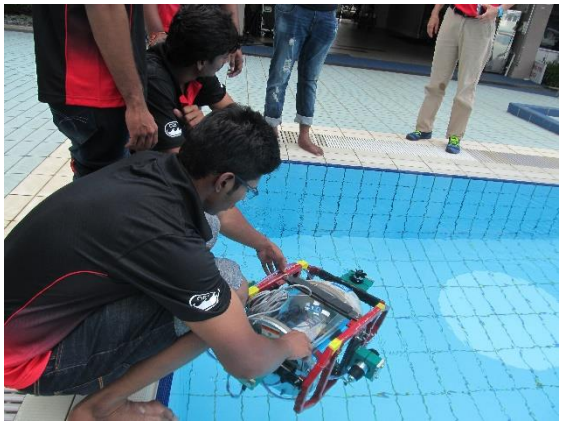

REFERENCES

1. Charles C. Eriksen et al., "Seaglider: A long-range autonomous underwater vehicle for oceanographic research", IEEE Journal of Oceanic Engineering, 2001, **Vol. 26, No.4**, October 2001.
2. Elgar desa, R. Madhan and P. Maurya, "Potential of autonomous underwater vehicles as new generation ocean data platforms", Current Science, 2006, **Vol. 90, No. 9**. 10th May 2006.
3. Pankajakshan, R., Remotigue, M.G., Taylor, L.K., Jiang, M., Briley, W.R. and Whitfield,D.L, "Validation of Control-Surface Induced Submarine Manoeuvring Simulations Using UNCLE", 24th Symposium on Naval Hydrodynamics,Fukuoka, Japan, July 8-13, 2002.
4. Thomas.C. Fu et al., "PIV measurements of the cross-flow wake of a turning submarine model (ONR body –1)", **NSWCCD-50-TR-2002 / 019** Hydromechanics Directorate Research and Development Report.
5. Yamamoto, I., Aoki, T., Tsukioka, S., Yoshida, H., Hyakudome, T., Sawa, T., Ishibashi, S., Inada, T., Yokoyama, K., Maeda, "Fuel cell system of auv 'Urashima", IEEE oceans/techno-ocean 2004.
6. Scott Kanowitz et al., "Subjugator: the development of an autonomous underwater vehicle", Machine Intelligence Laboratory,University of Florida, Gainesville, **Fl 32611.**
7. Yamamoto et al., "New discovery of marine system development", special

lecture, blue earth **'06,**Jamstec, Pacifico Yokohama, Japan, 2006.

8. Stevenson, Peter, Furlong, Maaten, Dormer, David, "AUV design: shape, drag and practical issues", Sea Technology, Jan 2009.

9. Davidson, Nielsen, P.V., and Sveningsson, "Modifications of the V2-f model for computing the flow in a 3d wall jet, Turbulence", Heat and Mass Transfer, 2003, **Vol.4**, pp. 577-584.

10. Zhen-yu Huang et al., "Calculations of flows over underwater appended bodies with high resolution eno schemes", 24th Symposium on Naval Hydrodynamics, Fukuoka, Japan, 8-13 July, 2002.

11. P.G. Esposito et al., "Numerical solutions of viscous flows about submerged and partly submerged bodies", Institute of Naval Studies and Experimental Architecture Naval. National academies press.

12. C.I. Yang, "Numerical simulation of three-dimensional viscous flow around a submersible body", David Taylor Research Center Bethesda, USA P-M. NASA Langley research center Hampton, USA.

13. P. Jagadeesh and K. Murali, "Investigations on alternative turbulence closure models for axisymmetric underwater hull forms", Journal Of Ocean Technology Maritime Emergency Management, **Vol. 1,** no. 2, 2006.

14. P. Jagadeesh and K. Murali, "Application of low-Re turbulence models for flow simulations past underwater vehicle hull forms", Journal of Naval Architecture and Marine Engineering,**Vol.1**, pp 41-54,2005.